# Catching Fullerenes: Synthesis of Molecular Nanogloves

Saber Mirzaei,[+#†] Xiangquan Hu,[+] M. Saeed Mirzaei,[+] Victor M. Espinoza Castro,[+] Xu Wang,[‡] Nicholas A. Figueroa,[÷] Tieyan Chang,[&] Ying-Pin Chen,[&] Gabriella Prieto Ríos,[#] Natalia Isabel Gonzalez-Pech,[÷≠] Yu-Sheng Chen,[&] and Raúl Hernández Sánchez[+#⊥*]

[+]Department of Chemistry, Rice University, 6100 Main St., Houston, Texas 77005, USA.

[#]Department of Chemistry, University of Pittsburgh, 219 Parkman Ave., Pittsburgh, Pennsylvania 15260, USA.

[‡]Shared Equipment Authority, Rice University, 6100 Main St., Houston, Texas 77005, USA.

[÷]Department of Chemistry, Hope College, Holland, Michigan 49423, USA.

[&]ChemMatCARS, The University of Chicago, Lemont, Illinois 60439, USA.

[⊥]Rice Advanced Materials Institute, Rice University, Houston, Texas 77005, USA.

**ABSTRACT:** Herein, we report the synthesis of a new series of rigid, all *meta*-phenylene, conjugated deep-cavity molecules, displaying high binding affinity towards buckyballs. A facile two-step synthetic approach with an overall yield of approximately 54% has been developed using a templating strategy that combines the general structure of resorcin[4]arene and [12]cyclo-*meta*-phenylene. These two moieties are covalently linked via four acetal bonds resulting in a glove-like architecture. $^1$H NMR titration experiments reveal fullerene binding affinities ($K_a$) exceeding $>10^6$ $M^{-1}$. The size complementarity between fullerenes and these scaffolds maximizes CH···π and π···π interactions and their host:guest adduct resemble a ball in a glove, hence their name as nanogloves. Fullerene recognition is tested by suspending carbon soot in a solution of nanoglove in 1,1,2,2-tetrachloroethane, where more than a dozen fullerenes are observed ranging from $C_{60}$ to $C_{96}$.

## INTRODUCTION

Macrocycles with well-defined shapes and cavities have been targeted as building blocks in nanoscience,[1] with applications spanning organic nanodevices,[2] host-guest chemistry,[3-4] sensors,[5-6] optoelectronic materials,[7] biomedical applications,[8-9] and several others.[10] Cyclophenylenes fall under the definition of conjugated macrocycles with an almost century-long history. Cyclo-*ortho*-phenylenes (COPs) were reported for the first time in the 1940's,[11-16] and later followed by cyclo-*meta*-phenylenes (CMPs) in the 1960's.[17-23] The radial nature of cyclo-*para*-phenylenes (CPPs) made them a challenging target for decades until their first report in 2008.[24-25] Moreover, the synthesis of cyclophenylenes with mixed connectivity, for example, integrating *meta*- and *para*-phenylenes within the same macrocycle, have been reported to create compounds with unique fluorescent properties and applications in cellular imaging.[26-27] The evolution of cyclophenylenes has paved the way to realize architectures that were previously only hypothetical, such as carbon nanobelts,[28-30] Möbius topologies,[31-33] and a large number of contorted aromatic compounds.[34-36]

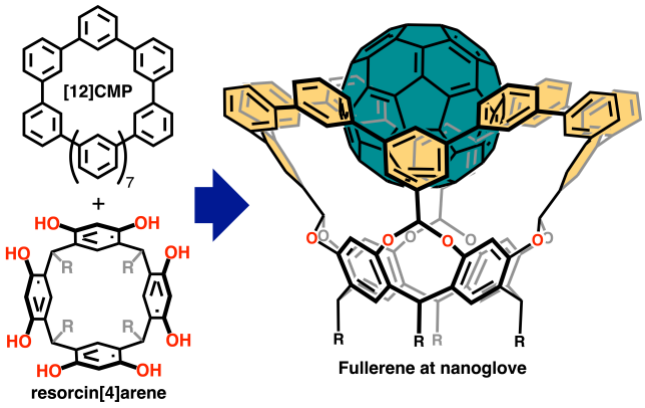


**Figure 1.** Nanoglove structure. The top section is a [12]CMP (yellow shade) while the bottom part is a resorcin[4]arene.

Macrocyclic arenes, such as calix[*n*]arenes, resorcin[*n*]arenes, calix[*n*]pyrroles, pillar[*n*]arenes, pyrogallo[*n*]arenes, and several others, have been active players for decades in establishing fundamental principles in supramolecular chemistry.[37] Lately, some of these families have been used in the formation of conjugated macrocycles as reported by Itami,[38-40] Chen,[41-42] Wang,[43] and Lucas.[44] Interested in merging ideas of conjugated and non-conjugated macrocycles, as demonstrated previously

with calix[*n*]arenes,[45] our group and others have been working on an approach using resorcin[*n*]arenes to template and direct the growth of conjugated architectures.[46-48] Advancing our previous work, we set out to incorporate [*n*]CMPs and resorcinarenes into a single scaffold. As a result, we obtained a class of compounds with a remarkable binding affinity for fullerenes, where the host-guest adduct resembles a ball in a baseball glove, thus we decided to call these architectures nanogloves (Figure 1). Herein, we report the synthetic methodology to obtain nanogloves, their full characterization, and their binding affinity and selectivity towards fullerenes.

## RESULTS AND DISCUSSION

### Synthesis

Nanogloves are obtained in high yields following a three-step synthesis from *n*-pentyl[49] or *n*-undecyl[50] resorcin[4]arene, $\mathbf{4_5}$ and $\mathbf{4_{11}}$, respectively (Figure 2a). These resorcinarenes were derivatized with 3,5-dibromo benzal bromide (**S1**) in anhydrous dimethylacetamide (DMA) under basic conditions using DBU (1,8-diazabicyclo[5.4.0]undec-7-ene),[51] to obtain $\mathbf{3_5}$ and $\mathbf{3_{11}}$ in 31 and 40% yield, respectively. Note that the gram-scale synthesis of $\mathbf{3_{11}}$ has been previously reported by Gibb and coworkers in 2007.[52] Suzuki–Miyaura cross coupling of $\mathbf{3_R}$ with 3-chlorophenyl boronic acid, or a substituted version containing a methyl or methoxy at the fifth position, results in $\mathbf{2X_R}$ (X= **a**, E = H; X= **b**, E = Me; X= **c**, E = OMe). The isolated yield of $\mathbf{2a_5}$ and $\mathbf{2a_{11}}$ is ~90%, which is remarkably high considering eight C–C bonds are formed in this step. The macrocyclization step towards $\mathbf{1X_R}$ was carried out in a nitrogen filled glovebox employing a Ni-mediated Yamamoto coupling. The reaction was performed using a 1:1 solvent mixture of toluene:DMF, 2,2'-bipyridine, and $Ni(cod)_2$, as the source of Ni(0), at 80 °C. Aside from $\mathbf{1a_5}$ which was isolated in 32% yield, all three other $\mathbf{1X_{11}}$ were obtained at around 60% isolated yield. Note that $\mathbf{1a_5}$ displays poor solubility in common organic solvents like $CHCl_3$ and $CH_2Cl_2$; hence, we focused on $\mathbf{1X_{11}}$ for subsequent studies. The structures of $\mathbf{1X_R}$ are expected to be rigid, thus its solubility profile is essentially dictated by its R group.

MALDI MS characterization of all three $\mathbf{1X_{11}}$ compounds showed a perfect match with their simulated isotopic patterns (Figure 2b). The $^1$H NMR of $\mathbf{1X_{11}}$ reveals their ideal $C_{4v}$ symmetry in solution (Figure 2c and Supporting

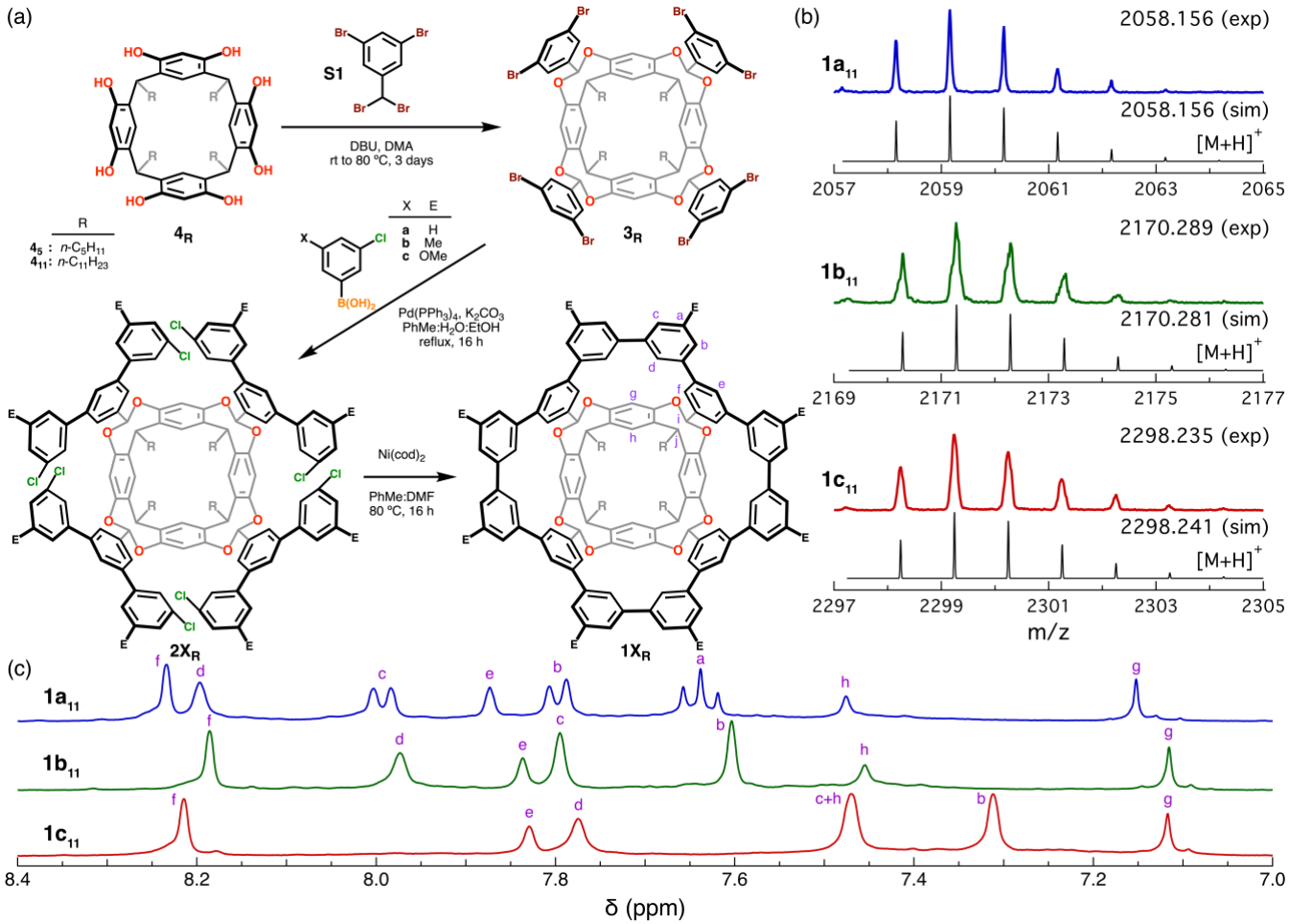


**Figure 2.** Synthesis and characterization of nanogloves. (a) Synthesis of $\mathbf{1X_R}$ starting from resorcin[4]arenes $\mathbf{4_5}$ and $\mathbf{4_{11}}$. (b) Experimental MALDI MS molecular ion peaks of $\mathbf{1X_{11}}$. Black traces represent simulations of $[M+H]^+$ isotopic distributions. (c) $^1$H NMR of $\mathbf{1a_{11}}$, $\mathbf{1b_{11}}$, and $\mathbf{1c_{11}}$ in 1,1,2,2-tetrachloroethane-$d_2$ at 20 °C. Proton labels according to (a). Note: in the synthesis of $\mathbf{2c_{11}}$, boronic acid pinacol ester was used instead of the free boronic acid. $\mathbf{1b_5}$ and $\mathbf{1c_5}$ were not synthesized.

Information). It is clear from Figure 2c how resonances "b", "c", and "d" shift upfield from **1a$_{11}$**, **1b$_{11}$**, to **1c$_{11}$** as the substituent becomes more electron donating. Last, an alternative method for the synthesis of **1X$_R$** consists of subjecting **3$_R$** to a cross coupling with the appropriate substituted biphenyl diboronic acid pinacol ester. To test this route, **3$_{11}$** and biphenyl-3,3'-diboronic acid bis(pinacol) ester were cross coupled under dilute conditions (See Supporting Information). The isolated yield of **1a$_{11}$** was 8% following this route. Therefore, the intermolecular approach to nanogloves is discouraged in favor of the intramolecular Yamamoto coupling.

### Structural Analysis

Single-crystal X-ray diffraction confirmed the glove-like structure of **1a$_5$**, **1b$_{11}$**, and **1c$_{11}$**. High quality single crystals were grown by slowly diffusing MeCN into chlorobenzene solutions of **1a$_5$**, **1b$_{11}$**, and **1c$_{11}$**. In addition to confirming the connectivity of **1a$_5$** (Figure 3), its crystal structure displays a cofacial dimeric nature in the solid state resulting from noncovalent CH···π interactions. Note that **1b$_{11}$** (Figure S20) and **1c$_{11}$** (Figure S21) have a different packing that does not involve a face-to-face interaction, likely because substituent E prevents it from happening.

The biphenyl moiety defined by rings A and A' in Figure 3 is relatively planar across **1a$_5$**, **1b$_{11}$**, and **1c$_{11}$** with dihedral angles of 16(4), 8(3), and 11(6) degrees, respectively. The planarity introduced into this biphenyl moiety is a direct result of the nanoglove architecture. To obtain quantitative information regarding the contraction introduced during nanoglove formation, the centroid of ring B was determined in all structures and the distance to the opposing centroid was extracted from the single-crystal X-ray diffraction data. Precursors **3$_5$** and **2a$_5$** display centroid-to-centroid distances of 12.7(6) and 12.70(5) Å, respectively, while nanogloves **1a$_5$**, **1b$_5$**, and **1c$_{11}$** exhibit only a small contraction to 11.7(3), 11.7(2), and 11.7(3) Å, respectively. The latter minor structural changes in centroid-to-centroid distance between precursors and nanogloves indicate that rigidification due to macrocyclization should result in an insignificant buildup of strain. In fact, based on the homodesmotic reaction in Figure S24 the strain energy of **1a$_1$** (R = Me) is ~9 kcal/mol (obtained by DFT at the B3LYP/6-31G(d) level of theory).[53]

### Electronic structure

The absorption and emission properties of nanogloves were investigated in dichloromethane to determine their electronic structure. All three nanogloves **1a$_{11}$**, **1b$_{11}$**, and **1c$_{11}$** have a well-defined main absorption band in the short-wave ultraviolet region, specifically at $\lambda_{max}$ of 254, 259, and 253 nm (Figure 4 left), respectively. This main absorption band is independent of the nature of substituent E and matches $\lambda_{max}$ for benzene (255 nm).[23] This similarity is expected due to destructive quantum interference resulting from the cross-conjugated nature of the twelve phenylene rings forming the outer rim of the nanoglove.[54-56] Additionally, a series of low energy weak absorption bands are unique in **1c$_{11}$** between 300 and 340 nm, with the lowest energy peak at ~330 nm.

The emission spectra for all three nanogloves **1a$_{11}$**, **1b$_{11}$**, and **1c$_{11}$** are nearly identical, showing an emission line centered at 342-343 nm (Figure 4 right). Interestingly, a second band is observed for **1c$_{11}$** at 354 nm. Time-dependent (TD) DFT calculations were used to investigate the nature of these electronic transitions. The major absorption bands are reproduced, albeit shifted to lower energies. For instance, major transitions around 280 – 300 nm were found in model compounds **1a$_1$** (282 nm, oscillator strength = $f \approx 0.27$), **1b$_1$** (285 nm, $f \approx 0.33$), and **1c$_1$** (299 nm, $f \approx 0.30$). A low energy transition in **1c$_1$** at 314 nm is calculated to correspond to H→L+2, which is attributed to one of the low energy bands observed in this compound (Table S2). In contrast to our previous reports[46-47] and [*n*]cyclo-*para*-phenylenes,[57-58] the HOMO-to-LUMO transition is not forbidden in nanogloves. For example, in **1a$_1$** the transition around 288 nm ($f \approx 0.04$) has a 55% contribution from the HOMO-to-LUMO transition, and similarly for **1b$_1$** and **1c$_1$** at 289 ($f \approx 0.07$, 64%) and 294 nm ($f \approx 0.05$, 34%), respectively.

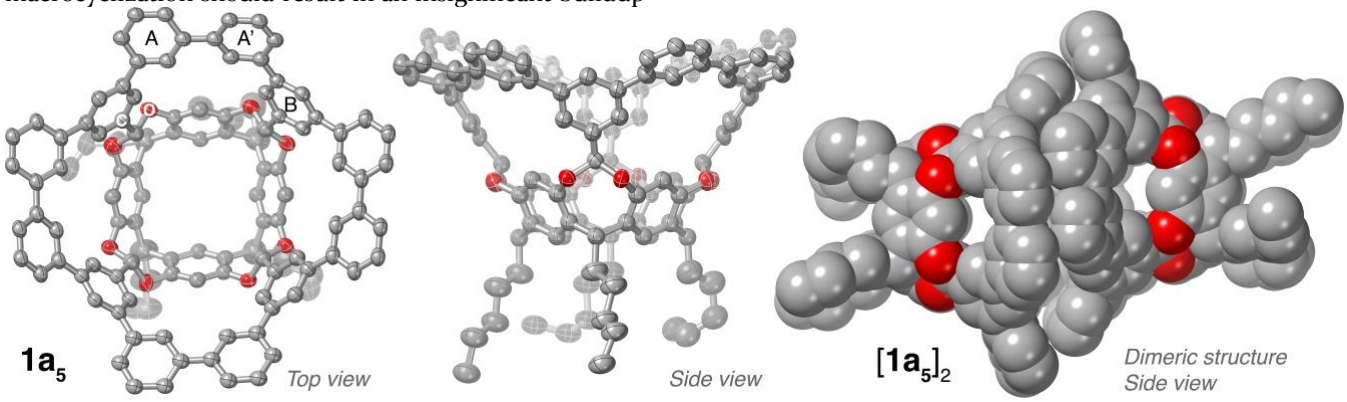


**Figure 3.** Molecular crystal structure of **1a$_5$** at 120 K. Thermal ellipsoids are shown at 50% probability level. The dimeric structure of **1a$_5$** is shown to the right in the sphere packing model.

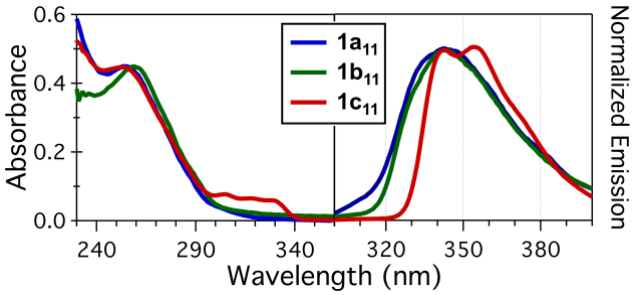


**Figure 4**. (*Left*) Absorption and (*right*) emission bands of nanogloves collected in $CH_2Cl_2$ at room temperature.

To understand why the HOMO-to-LUMO transition is not forbidden, as it is in other conjugated macrocycles,[59] we evaluated the frontier molecular orbitals (FMOs) of nanogloves. Depicted in Figure S26 to S28 are the HOMO and LUMO for **1a**$_1$, **1b**$_1$, and **1c**$_1$. In contrast to [*n*]CPPs, where the HOMO and LUMO reside uniformly across the conjugated nanoring,[60] the HOMO and LUMO are not evenly distributed across the [12]CMP fragment of the nanoglove. In fact, the asymmetry in the orbital distribution is more apparent as the electron donation ability of the substituent E increases. Looking at the HOMO, both **1a**$_1$ and **1b**$_1$ display a benzenoid character in the biphenyl fragment composed of rings A and A', while **1c**$_1$ exhibits a quinoid shape.

### Catching Fullerenes

Fullerenes have a unique spheroidal π conjugated surface. Receptors for fullerenes capable of establishing host:guest adducts have been explored since the discovery of $C_{60}$.[61] A non-exhaustive list of fullerene receptors includes molecular tweezers,[62-64] carbon nanohoops,[65] phenine nanotubes,[66] metallosupramolecular receptors,[67-68] (metallo)porphyrins,[69-73] molecular organic cages,[74-76] corannulene hosts,[77] adaptable macrocycles,[78] calix[*n*]arenes,[79] cavitands,[80-81] and metal-organic frameworks.[82-83] Most of these hosts stabilize fullerenes through concave-convex π-π interactions.[84-86] Almost all of the previous receptors were purposely designed to bind fullerenes; however, some macrocyclic arenes, like those introduced earlier in this manuscript, have been found to encapsulate fullerenes due to their basket-like structure. Examples include cyclotriveratrylene (CTV),[87-88] calix[*n*]arenes,[89-90] and pillar[*n*]arenes.[91] Most of these macrocycles display weak binding towards fullerenes in solution (<$10^3$ $M^{-1}$)[91] or they only form adducts in the solid state by benefiting from the size complementarity.[92-93] Most relevant, molecules with spherical or pseudospherical geometries able to encapsulate $C_{60}$ are rather rare.[94-95]

We hypothesized that nanogloves would have the ability to host fullerenes due to their bowl-shaped structure. The binding affinity of $C_{60}$ for **1a**$_{11}$ was tested using $^1$H NMR in 1,1,2,2-tetrachloroethane-$d_2$ (TCE-$d_2$). The NMR solvent was chosen to maximize the solubility of $C_{60}$,[96] while maintaining **1a**$_{11}$ in solution. Upon titration of $C_{60}$ into **1a**$_{11}$, the resonance of the acetal hydrogen, labeled as "i", shifted from 5.62 to 5.41 ppm (Figure 5a). As the titration proceeds forward, both free **1a**$_{11}$ and $C_{60}\subset$**1a**$_{11}$ co-exist indicating that the equilibrium established during adduct formation strongly favored the host-guest complex species $C_{60}\subset$**1a**$_{11}$ with an association constant ($K_a$) surpassing the limit measurable by NMR (>$10^6$ $M^{-1}$).[97] Observing that resonance "i" shifts upfield, we find literature reports indicating that aromatic C–H bonds move upfield as π-π stacking increases.[98-99] However, in our case, it is an acetal C–H

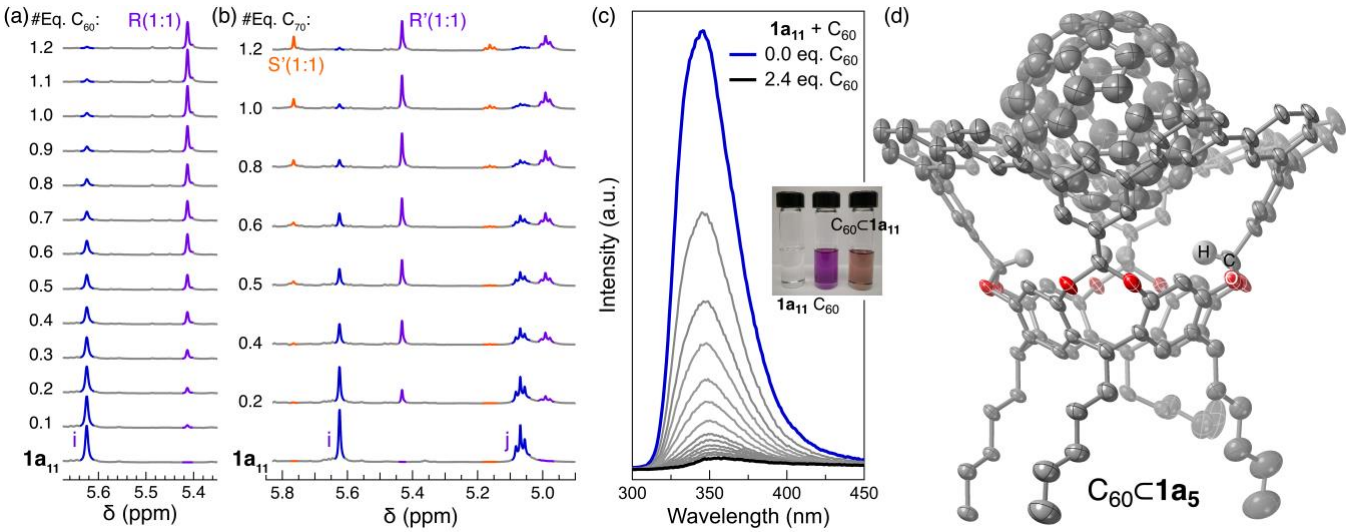


**Figure 5**. Fullerene binding to nanogloves. $^1$H NMR titration of (a) $C_{60}$ and (b) $C_{70}$ into **1a**$_{11}$ in 1,1,2,2-tetrachloroethane-$d_2$ (TCE-$d_2$) at 20 °C. The 1:1 host:guest adducts R(1:1) and R'(1:1) are highlighted in purple traces, while S'(1:1) is shown in orange. Resonances "i" and "j" are labeled according to Figure 2. (c) Fluorescence quenching titration of **1a**$_{11}$ with $C_{60}$ in TCE at room temperature. Inset: photographic images of solutions of **1a**$_{11}$, $C_{60}$, and $C_{60}\subset$**1a**$_{11}$ in TCE under ambient light. (d) Molecular crystal structure of $C_{60}\subset$**1a**$_5$ at 100 K. Thermal ellipsoids are shown at 50% probability level. C and O are shown in grey and red, respectively.

bond pointing at $C_{60}$. Computational studies indicate a shielding effect above the hexagonal rings in $C_{60}$ and $C_{70}$, and deshielding when above the pentagons.[100] Previous reports show a net deshielding effect,[101] while in our case a net shielding of the acetal C–H is observed. Furthermore, as more equivalents of $C_{60}$ are added, the acetal resonance shifts completely to the upfield position producing a 1:1 adduct ($C_{60}\subset$**1a**$_{11}$) that we labeled R(1:1) in Figure 5a. An identical behavior is observed when **1b**$_{11}$ (Figure S30) and **1c**$_{11}$ (Figure S31) are titrated with $C_{60}$.

Titration experiments involving $C_{70}$ presented an additional intricacy. As shown in Figure 5b, titration of $C_{70}$ into **1a**$_{11}$ produces a mixture of two host guest adducts R'(1:1) and S'(1:1). The acetal resonance in R'(1:1) is upfield shifted and at the same chemical shift as R(1:1), in contrast resonance "i" in S'(1:1) shifts downfield to 5.76 ppm (full spectrum in Figure S32). Interestingly, when $C_{70}$ is titrated to **1b**$_{11}$ (Figure S33) or **1c**$_{11}$ (Figure S34) the only adduct formed is S'(1:1). Free nanoglove resonances disappear when one equivalent of $C_{70}$ is added to **1b**$_{11}$ or **1c**$_{11}$ producing the host:guest complexes $C_{70}\subset$**1b**$_{11}$ or $C_{70}\subset$**1c**$_{11}$. In comparison, when ca. 1 equivalent of $C_{70}$ is added to **1a**$_{11}$, resonance "i" for free **1a**$_{11}$ disappears and gives rise to R'(1:1) and S'(1:1) at a ratio of 2 to 1, respectively. Given the ovoidal shape of $C_{70}$, we hypothesized that end-on and side-on adducts were possible. The structures of these species were optimized via DFT methods, and their relative energies were obtained at the B3LYP-D3BJ/6-31G* level of theory. The $C_{70}$ end-on adduct with **1a**$_{11}$ is shown in Figure S35 left. In the end-on adduct, $C_{70}$'s reach within the nanoglove pocket is similar to when $C_{60}$ is hosted within **1a**$_{11}$. Based on this similarity and the fact that hexagons are above the acetal hydrogen, we expect both to produce an upfield shift of the acetal resonance. Hence, we designate the end-on adduct as R'(1:1). The optimized structure of the side-on adduct is shown in Figure S35 right and is calculated to be 2.4 kcal/mol higher in energy than R'(1:1).

Intrigued by the strong binding of fullerenes to nanogloves, we carried out fluorescence quenching experiments to obtain quantitative binding data. A representative example is shown in Figure 5c, where $C_{60}$ is titrated to **1a**$_{11}$ and the evolution of the emission band at 342 nm is recorded as titration proceeds from 0 to 2.4 equivalents of $C_{60}$. All titration experiments of $C_{60}$ and $C_{70}$ into **1X**$_{11}$ are shown in Figures S36 to S38. All data was analyzed using Bindfit[102] for a 1:1 host:guest model. Note that individual association constants ($K_a$'s) towards R'(1:1) and S'(1:1) cannot be obtained via fluorescence quenching and instead are merged into a single value. Interestingly, $K_a$ values across all six titrations, $C_{60}$ and $C_{70}$ into **1X**$_{11}$, fluctuate around 1-to-3 × $10^7$ $M^{-1}$ in TCE at room temperature. The strong fullerene association observed within nanogloves is larger or comparable to the strongest host:fullerene adducts reported in the literature.[67, 103-105] Also, opposite to binding of $C_{70}$, $C_{60}$ encapsulation can be readily detected with the naked eye as the colorless host solution of **1a**$_{11}$ changes to brown with incremental addition of the purple solution of $C_{60}$ (Figure 5c inset). Strong binding of fullerenes facilitated the formation of high-quality single crystals by slow diffusion of MeCN into $C_{60}\subset$**1a**$_5$ in *ortho*-dichlorobenzene (*o*-DCB). The molecular crystal structure of $C_{60}\subset$**1a**$_5$ displays the fullerene perfectly nested within the nanoglove (Figure 5d and S39). The average distance between the acetal hydrogen and the closest carbon atom at $C_{60}$ is 2.91(3) Å. This short distance indicates a strong C–H•••π interaction according to literature values.[106] Moreover, π–π interactions are also operative as determined from the short average distance of 3.31(7) Å between the centroid of ring B (Figure 3) and the closest carbon atom or ring centroid at $C_{60}$.[107] DFT calculations using the independent gradient model based on Hirshfeld partition of molecular density (IGMH) provide a visualization of the non-covalent interaction surface between $C_{60}$ and **1a**$_1$ (Figure S40).[108] The bowl-shape of this interaction surface demonstrates the

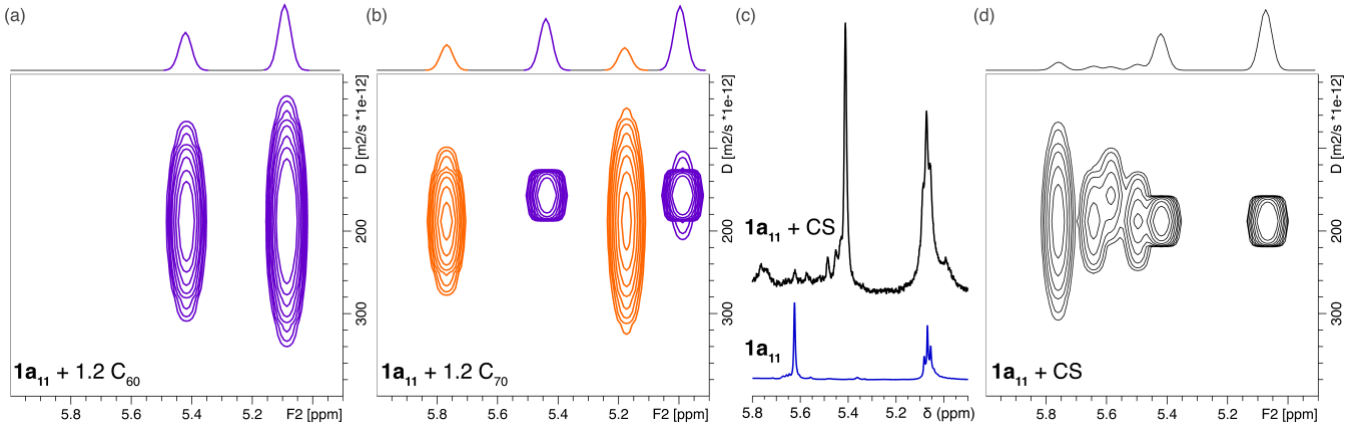


**Figure 6.** Diffusion of host:guest adducts and extraction of fullerenes by **1a**$_{11}$ from carbon soot. Acetal (resonance "i") and methine (resonance "j") region of DOSY NMR of (a) $C_{60}\subset$**1a**$_{11}$ and (b) $C_{70}\subset$**1a**$_{11}$. The R(1:1) adduct is shown in purple in (a), while (b) displays the mixture of S'(1:1) and R'(1:1) in orange and purple, respectively. (c) $^1$H NMR of acetal region of **1a**$_{11}$ (blue) and the extracted adducts obtained by subjecting carbon soot (CS) to **1a**$_{11}$ (black) in TCE. (d) DOSY NMR of extract from **1a**$_{11}$ + CS shown in (c). All NMR data was collected in TCE-$d_2$.

excellent nesting pocket provided by nanogloves **1X$_{11}$**. Last, the overall geometry of **1a$_5$** remains unchanged upon host-guest adduct formation suggesting a negligible penalty towards reorganizational energy resulting in enhanced binding affinity constants.[109-110]

Understanding the solution transport properties of fullerenes is essential for developing new strategies for their separation and purification.[86, 111] The diffusion coefficient (*D*) is one of the fundamental parameters of interest and it is commonly determined through DOSY NMR spectroscopy.[112] For $C_{60}$ and $C_{70}$, *D* has been determined in a variety of solvents with different viscosities ($\eta$) and it ranges from 1-to-9 × $10^{-10}$ $m^2/s$.[113] Specifically, *D* for $C_{60}$ in *o*-DCB ($\eta$ = 1.32) and benzonitrile ($\eta$ = 1.24) is 1.1(2) × $10^{-10}$ and 1.4(3) × $10^{-10}$ $m^2/s$, respectively, which we assume to be close to that in TCE ($\eta$ = 1.43) based on their similar viscosity properties.[114] In host:guest complexes, DOSY NMR can only be reliably applied to adducts existing in the slow exchange regime,[115] which is the case here as established in Figure 5a-b. Examining DOSY NMR of R(1:1), $C_{60}\subset$**1a$_{11}$**, we observe a diffusion coefficient of ca. 2 × $10^{-10}$ $m^2/s$ (Figure 6a). Similarly, R'(1:1) and S'(1:1) behave nearly the same as R(1:1), suggesting that the diffusion properties are not influenced by how $C_{70}$ is hosted within **1a$_{11}$** (Figure 6b). Overall, these findings follow expected trends obtained by others correlating *D* and molecular weight.[116-117]

Fullerene availability is hindered by challenging separation and purification procedures.[111, 118] Fullerene-rich carbon soots (CSs) are available commercially containing ~5% fullerenes.[119] However, additional information about the specific fullerenes present, aside from $C_{60}$ and $C_{70}$, is not disclosed. We hypothesized that fullerenes may bind to nanogloves even if they were present in complex mixtures. To test this hypothesis, CS was suspended in a solution of **1a$_{11}$** in TCE at 100 °C for 12 hours (detailed procedure in Supporting Information). The suspension was filtered, and the resulting solution was dried under reduced pressure. Since the acetal and methine resonances "i" and "j", respectively, are sensitive to the formation of fullerene⊂nanoglove adducts, the filtrate was subjected to $^1$H NMR analysis in TCE-$d_2$ to search for potential fullerene complexes. The region of the $^1$H NMR spectrum from 4.9 to 5.8 ppm displays multiple resonances suggesting a variety of fullerene adducts (Figure 6c, black trace). The major resonances coincide with R(1:1) and R'(1:1); however, several more are discernible that are not related to adducts of $C_{60}$ or $C_{70}$. Furthermore, analysis of the CS filtrate by DOSY NMR (Figure 6d) suggests that all fullerene adducts formed in solution must be 1:1 host:guest as they are clustered around R(1:1), R'(1:1), and S'(1:1). The likelihood of 1:2 adducts in solution is discarded as these would increase the hydrodynamic radii of the diffusing species and result in a lower value of *D* compared to the 1:1 complex. For reference, the adduct $C_{60}\subset$(**1a$_1$**)$_2$ is almost twice as long as $C_{60}\subset$**1a$_1$** (Figure S41). Last, despite observing multiple fullerene adducts via NMR their exact molecular identity was not established.

MALDI MS was used to identify the fullerenes obtained from carbon soot. We collected data up to m/z = 9000 showing three distinct m/z regions: the first one near 3000, a second one in and around 5000, and a third one at 7000 (Figure S42a). Note that free **1a$_{11}$** is not observed (m/z = 2058, Figure 2b). Rather surprisingly, the first region only displays a single species corresponding to $[C_{60}\subset$**1a$_{11}$**$]^-$ (Figure 7a). In contrast, the second region contains a multitude of ion peaks, where the major ones correspond to $[C_{60}\subset$(**1a$_{11}$**)$_2]^-$ and $[C_{70}\subset$(**1a$_{11}$**)$_2]^-$ (Figure 7b). Detailed analysis of the minor ion peak distributions between m/z = 4850 and 5300 reveals the formation of $[C_n\subset$(**1a$_{11}$**)$_2]^-$ for n = 64, 66, 74, 76, 78, and 82 to 96 every two units (Figure 7c). Note that while most of these adducts match their isotopic distribution considering $C_n$ alone, others are off by several units indicating potential functionalization. Recently,

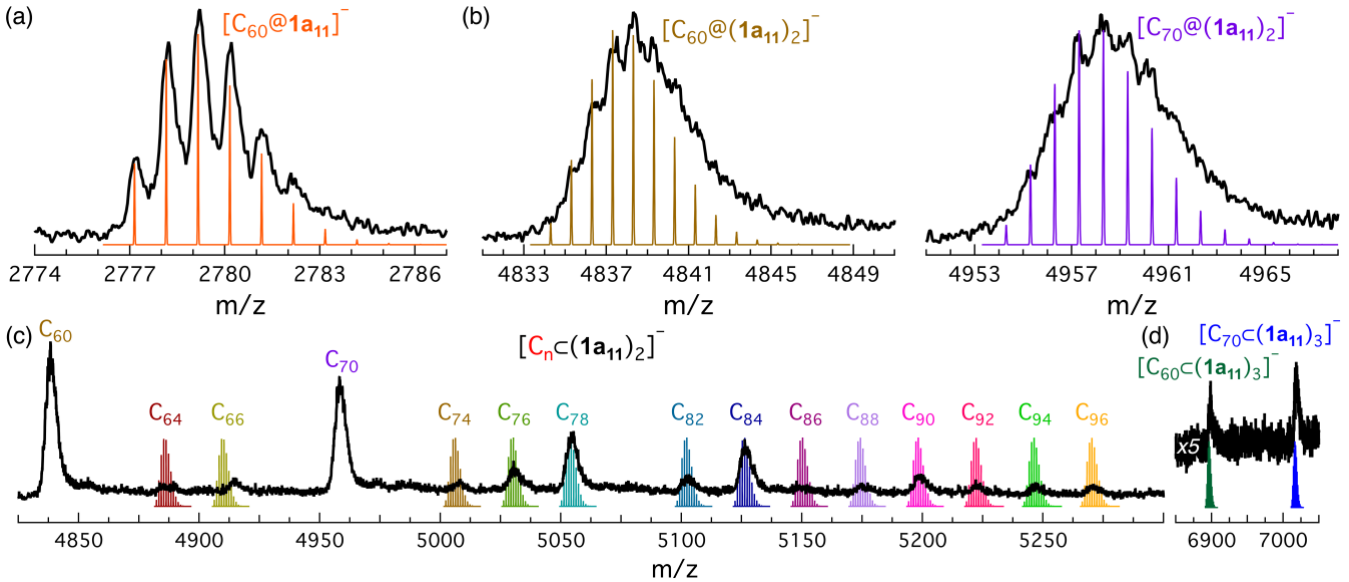


**Figure 7.** MALDI MS of carbon soot (CS) filtrate. CS was suspended with **1a$_{11}$** dissolved in TCE at 100 °C.

Yamada, Akasaka, and Nagase highlighted that anomalous carbon cages are present in carbon soot.[120] Aside from $C_{60}$ and $C_{70}$, using nanoglove **1a$_{11}$** we observe the adduct $[C_n \subset (\mathbf{1a_{11}})_2]^-$ with $C_{64}$ and a closely related species. Aside from its allotropic form, $C_{64}$ has been isolated as $C_{64}H_4$,[121] $C_{64}Cl_4$,[122] or $C_{64}Cl_8$;[123] similarly, $C_{66}$ has been obtained as $C_{66}H_4$.[124] In both of these cases a closely related carbon cage heavier than the pure $C_{64}$ and $C_{66}$ must be present. The last two species in the series $C_{74}$, $C_{76}$, and $C_{78}$ match well to the pure allotrope sandwiched between two nanogloves; however, the experimental pattern does not fit entirely well for $[C_{74} \subset (\mathbf{1a_{11}})_2]^-$, likely indicating an unknown $C_{74}$ cage. Functionalization precedents for these three species are known in the form of $C_{74}C_{10}$,[125] $C_{76}Cl_{18}$,[126] $C_{76}Cl_{24}$,[127] and $C_{78}Cl_{18}$.[128] The host:guest compound $[C_{80} \subset (\mathbf{1a_{11}})_2]^-$ is not observed in the mass spectrum in Figure 7. Its absence is not entirely surprising as it is known to exist in low abundance in soot.[129] Fullerene $C_{82}$ and $C_{84}$ match well the simulated isotopic pattern for $[(C_{82}$ or $C_{84}) \subset (\mathbf{1a_{11}})_2]^-$. In contrast, $C_{86}$ and $C_{88}$ are barely noticeable in the mass spectrum despite having several stable isomers.[130–132] Fullerene $C_{90}$, and larger, have been reported to adopt tubular-like structures,[133] and more recently categorized as fullertubes.[134–135] Our data does not allow us to discern the nature of the isomer(s) extracted from CS; however, based on data presented vide supra, isomers with end-caps having $C_{60}$-like structures will nest better within **1X$_{11}$** and form favorable host:guest adducts. Furthermore, the simulated isotopic patterns for $[C_n \subset (\mathbf{1a_{11}})_2]^-$ with $C_{92}$, $C_{94}$, and $C_{96}$[136] match well the experimental MS data. Finally, the third region at around m/z = 7000 shows ion peaks matching the adducts $[C_n \subset (\mathbf{1a_{11}})_3]^-$ for $C_{60}$ and $C_{70}$ (Figure 7d). This is somewhat unexpected suggesting the third equivalent probably wraps around the ternary adduct $[C_n \subset (\mathbf{1a_{11}})_2]^-$ as a stitch. Finally, comparing mass spectra data of CS in the presence and absence of nanogloves demonstrates preferential detection of fullerenes when **1a$_{11}$** is present, especially for congeners heavier than $C_{70}$ (Figure S43).

## CONCLUSIONS

Following on our synthetic strategy to make contorted aromatic species, here we report the efficient access to molecules with deep cavities coined nanogloves. Employing resorcin[4]arene as the template, and two subsequent coupling reactions, we disclose a series of nanogloves with exceptional binding affinities for buckyballs. The top rim represents a [12]CMP structure which is covalently linked to the template via four benzal C–C bonds. The high binding constants of fullerenes to nanogloves are attributed to their rigid structure allowing them to establish a surface of non-covalent π···π contacts and CH···π interactions with the nested buckyball. Moreover, we exploit fullerene's high binding affinities towards nanogloves to selectively sequester them from carbon soot. This work may lead the way to the synthesis of unprecedented structures and materials to use in fullerene purification, their regioselective functionalization, and fullerene solubilization for their availability in standard organic solvents.

## ASSOCIATED CONTENT

### Supporting Information

The Supporting Information is available free of charge on the ACS Publications website.

Experimental details, materials and methods including DFT calculations, single-crystal X-ray diffraction data, multinuclear NMR spectra, light absorption and emission spectra, and MS data.

## AUTHOR INFORMATION


### Corresponding Author

*Raúl Hernández Sánchez – Department of Chemistry, Rice University, 6100 Main St., Houston, Texas 77005, USA; Rice Advanced Materials Institute, Rice University, Houston, Texas 77005, USA.

### Present Addresses

†Saber Mirzaei. Department of Chemistry, University of California, Berkeley, California 94720, United States.

≠Natalia Isabel Gonzalez-Pech. Department of Chemistry, Wesleyan University, Middletown, Connecticut 06459, United States.


### Author Contributions

All authors contributed to the discussion of the results and the final manuscript preparation.


### Funding Sources

This research was partially supported by the National Science Foundation NSF CAREER CHE-2302628. This research was supported with startup funds by Rice University and the University of Pittsburgh. We thank Dr. Christopher L. Pennington for assistance with HRMS data collection. R.H.S. acknowledges the support of the Robert A. Welch Foundation Young Investigator Award. This research was funded in part by a grant from The Welch Foundation (C-2142-20230405). NSF's ChemMatCARS, Sector 15 at the Advanced Photon Source (APS), Argonne National Laboratory (ANL) is supported by the Divisions of Chemistry (CHE) and Materials Research (DMR), National Science Foundation, under grant number NSF/CHE-1834750 and NSF/CHE-2335833 This research used resources of the Advanced Photon Source; a U.S. Department of Energy (DOE) Office of Science user facility operated for the DOE Office of Science by Argonne National Laboratory under Contract No. DE-AC02-06CH11357.


### Notes

The authors declare no competing financial interest.

## ACKNOWLEDGMENT


We thank the support from the Center for Research Computing at the University of Pittsburgh. S.M. acknowledges the support from the Dietrich School of Arts & Sciences Graduate Fellowship and the Andrew Mellon Pre-doctoral Fellowship. This research was supported through

instrumentation made available through the Shared Instrumentation Authority at Rice University.

## REFERENCES


1. Iyoda, M.; Yamakawa, J.; Rahman, M. J., Conjugated Macrocycles: Concepts and Applications. *Angew. Chem. Int. Ed.* **2011,** *50* (45), 10522-10553.
2. Zang, L.; Che, Y.; Moore, J. S., One-Dimensional Self-Assembly of Planar π-Conjugated Molecules: Adaptable Building Blocks for Organic Nanodevices. *Acc. Chem. Res.* **2008,** *41* (12), 1596-1608.
3. Leonhardt, E. J.; Jasti, R., Emerging applications of carbon nanohoops. *Nat. Rev. Chem.* **2019,** *3* (12), 672-686.
4. Lu, D.; Huang, Q.; Wang, S.; Wang, J.; Huang, P.; Du, P., The Supramolecular Chemistry of Cycloparaphenylenes and Their Analogs. *Front. Chem.* **2019,** *7* (668).
5. Duan, Q.; Wang, F.; Lu, K., Recent advances in macrocyclic arenes-based fluorescent indicator displacement assays. *Front. Chem.* **2022,** *10*.
6. Li, X.; Jin, Y.; Zhu, N.; Yin, J.; Jin, L. Y., Recent Developments of Fluorescence Sensors Constructed from Pillar[n]arene-Based Supramolecular Architectures Containing Metal Coordination Sites. *Sensors* **2024,** *24* (5).
7. Ball, M.; Zhang, B.; Zhong, Y.; Fowler, B.; Xiao, S.; Ng, F.; Steigerwald, M.; Nuckolls, C., Conjugated Macrocycles in Organic Electronics. *Acc. Chem. Res.* **2019,** *52* (4), 1068-1078.
8. Zhang, H.; Ma, X.; Nguyen, K. T.; Zhao, Y., Biocompatible Pillararene-Assembly-Based Carriers for Dual Bioimaging. *ACS Nano* **2013,** *7* (9), 7853-7863.
9. Sathiyajith, C.; Shaikh, R. R.; Han, Q.; Zhang, Y.; Meguellati, K.; Yang, Y.-W., Biological and related applications of pillar[n]arenes. *Chem. Commun.* **2017,** *53* (4), 677-696.
10. Han, X.-N.; Han, Y.; Chen, C.-F., Recent advances in the synthesis and applications of macrocyclic arenes. *Chem. Soc. Rev.* **2023,** *52* (9), 3265-3298.
11. Rapson, W. S.; Shuttleworth, R. G.; van Niekerk, J. N., 89. Benzcyclooctatetraenes. Part III. Diphenylene and tetraphenylene. *J. Chem. Soc.* **1943,** (0), 326-327.
12. Karle, I. L.; Brockway, L. O., The Structures of Biphenyl, o-Terphenyl and Tetraphenylene1. *J. Am. Chem. Soc.* **1944,** *66* (11), 1974-1979.
13. Ernst, L.; Mannschreck, A.; Rümpler, K.-D., Proton magnetic resonance spectra of the atropisomers of ortho-hexaphenylene. *Org. Magn. Reson.* **1973,** *5* (3), 125-128.
14. Wuckert, E.; Hägele, C.; Giesselmann, F.; Baro, A.; Laschat, S., Saddle-shaped tetraphenylenes with peripheral gallic esters displaying columnar mesophases. *Beilstein J. Org. Chem.* **2009,** *5*, 57.
15. Huang, H.; Hau, C.-K.; Law, C. C. M.; Wong, H. N. C., Hydroxytetraphenylenes, a new type of self-assembling building block and chiral catalyst. *Org. Biomol. Chem.* **2009,** *7* (7), 1249-1257.
16. Rajca, A.; Rajca, S., Asymmetric Synthesis of Chiral Tetraphenylenes. *Angew. Chem. Int. Ed.* **2010,** *49* (4), 672-674.
17. Staab, H. A.; Binnig, F., Synthese Und Eigenschaften Von Hexa-Meta-Phenylen. *Tetrahedron Lett.* **1964,** (7-8), 319-321.
18. Staab, H. A.; Binnig, F., Zur Konjugation in makrocyclischen Bindungssystemen, VII. Synthese und Eigenschaften von Hexa-m-phenylen und Octa-m-phenylen. *Chem. Ber.* **1967,** *100* (1), 293-305.
19. Cram, D. J.; Kaneda, T.; Helgeson, R. C.; Lein, G. M., Spherands - ligands whose binding of cations relieves enforced electron-electron repulsions. *J. Am. Chem. Soc.* **1979,** *101* (22), 6752-6754.
20. Cram, D. J.; Kaneda, T.; Helgeson, R. C.; Brown, S. B.; Knobler, C. B.; Maverick, E.; Trueblood, K. N., Host-guest complexation. 35. Spherands, the first completely preorganized ligand systems. *J. Am. Chem. Soc.* **1985,** *107* (12), 3645-3657.
21. Pisula, W.; Kastler, M.; Yang, C.; Enkelmann, V.; Müllen, K., Columnar Mesophase Formation of Cyclohexa-m-phenylene-Based Macrocycles. *Chem. Asian J.* **2007,** *2* (1), 51-56.
22. Chan, J. M. W.; Swager, T. M., Synthesis of arylethynylated cyclohexa-m-phenylenes via sixfold Suzuki coupling. *Tetrahedron Lett.* **2008,** *49* (33), 4912-4914.
23. Xue, J. Y.; Ikemoto, K.; Takahashi, N.; Izumi, T.; Taka, H.; Kita, H.; Sato, S.; Isobe, H., Cyclo-meta-phenylene Revisited: Nickel-Mediated Synthesis, Molecular Structures, and Device Applications. *J. Org. Chem.* **2014,** *79* (20), 9735-9739.
24. Jasti, R.; Bhattacharjee, J.; Neaton, J. B.; Bertozzi, C. R., Synthesis, Characterization, and Theory of [9]-, [12]-, and [18]Cycloparaphenylene: Carbon Nanohoop Structures. *J. Am. Chem. Soc.* **2008,** *130* (52), 17646-17647.
25. Lewis, S. E., Cycloparaphenylenes and related nanohoops. *Chem. Soc. Rev.* **2015,** *44* (8), 2221-2304.
26. Lovell, T. C.; Colwell, C. E.; Zakharov, Lev N.; Jasti, R., Symmetry breaking and the turn-on fluorescence of small, highly strained carbon nanohoops. *Chem. Sci.* **2019,** *10* (13), 3786-3790.
27. Lovell, T. C.; Bolton, S. G.; Kenison, J. P.; Shangguan, J.; Otteson, C. E.; Civitci, F.; Nan, X.; Pluth, M. D.; Jasti, R., Subcellular Targeted Nanohoop for One- and Two-Photon Live Cell Imaging. *ACS Nano* **2021,** *15* (9), 15285-15293.
28. Bergman, H. M.; Kiel, G. R.; Handford, R. C.; Liu, Y.; Tilley, T. D., Scalable, Divergent Synthesis of a High Aspect Ratio Carbon Nanobelt. *J. Am. Chem. Soc.* **2021,** *143* (23), 8619-8624.
29. Zhu, J.; Han, Y.; Ni, Y.; Li, G.; Wu, J., Facile Synthesis of Nitrogen-Doped $[(6.)_m8]_n$Cyclacene Carbon Nanobelts by a One-Pot Self-Condensation Reaction. *J. Am. Chem. Soc.* **2021,** *143* (7), 2716-2721.
30. Li, Y.; Kono, H.; Maekawa, T.; Segawa, Y.; Yagi, A.; Itami, K., Chemical Synthesis of Carbon Nanorings and Nanobelts. *Acc. Mater. Res.* **2021,** *2* (8), 681-691.
31. Segawa, Y.; Watanabe, T.; Yamanoue, K.; Kuwayama, M.; Watanabe, K.; Pirillo, J.; Hijikata, Y.; Itami, K., Synthesis of a Möbius carbon nanobelt. *Nature Synth.* **2022,** *1* (7), 535-541.
32. Nishigaki, S.; Shibata, Y.; Nakajima, A.; Okajima, H.; Masumoto, Y.; Osawa, T.; Muranaka, A.; Sugiyama, H.; Horikawa, A.; Uekusa, H.; Koshino, H.; Uchiyama, M.; Sakamoto, A.; Tanaka, K., Synthesis of Belt- and Möbius-Shaped Cycloparaphenylenes by Rhodium-Catalyzed Alkyne Cyclotrimerization. *J. Am. Chem. Soc.* **2019,** *141* (38), 14955-14960.
33. Naulet, G.; Sturm, L.; Robert, A.; Dechambenoit, P.; Röhricht, F.; Herges, R.; Bock, H.; Durola, F., Cyclic tris-[5]helicenes with single and triple twisted Möbius topologies and Möbius aromaticity. *Chem. Sci.* **2018,** *9* (48), 8930-8936.
34. Fan, W.; Matsuno, T.; Han, Y.; Wang, X.; Zhou, Q.; Isobe, H.; Wu, J., Synthesis and Chiral Resolution of Twisted Carbon Nanobelts. *J. Am. Chem. Soc.* **2021,** *143* (39), 15924-15929.
35. Guo, Q.-H.; Qiu, Y.; Wang, M.-X.; Fraser Stoddart, J., Aromatic hydrocarbon belts. *Nat. Chem.* **2021,** *13* (5), 402-419.
36. Krzeszewski, M.; Ito, H.; Itami, K., Infinitene: A Helically Twisted Figure-Eight [12]Circulene Topoisomer. *J. Am. Chem. Soc.* **2022,** *144* (2), 862-871.
37. Wu, J.-R.; Yang, Y.-W., New opportunities in synthetic macrocyclic arenes. *Chem. Commun.* **2019,** *55* (11), 1533-1543.
38. Li, Y.; Segawa, Y.; Yagi, A.; Itami, K., A Nonalternant Aromatic Belt: Methylene-Bridged [6]Cycloparaphenylene Synthesized from Pillar[6]arene. *J. Am. Chem. Soc.* **2020,** *142* (29), 12850-12856.
39. Kai, N.; Kono, H.; Yagi, A.; Itami, K., Synthesis and Properties of Methylene-Bridged [6]Cyclo-2,6-naphthylene. *Synlett* **2023,** *34* (12), 1433-1436.
40. Kono, H.; Li, Y.; Zanasi, R.; Monaco, G.; Summa, F. F.; Scott, L. T.; Yagi, A.; Itami, K., Methylene-Bridged [6]-, [8]-, and [10]Cycloparaphenylenes: Size-Dependent Properties and Paratropic Belt Currents. *J. Am. Chem. Soc.* **2023,** *145* (16), 8939-8946.
41. Du, X.-S.; Zhang, D.-W.; Guo, Y.; Li, J.; Han, Y.; Chen, C.-F., Towards the Highly Efficient Synthesis and Selective Methylation of C($sp^3$)-Bridged [6]Cycloparaphenylenes from Fluoren[3]arenes. *Angew. Chem. Int. Ed.* **2021,** *60* (23), 13021-13028.
42. Zhang, F.; Du, X.-S.; Zhang, D.-W.; Wang, Y.-F.; Lu, H.-Y.; Chen, C.-F., A Green Fluorescent Nitrogen-Doped Aromatic Belt Containing a [6]Cycloparaphenylene Skeleton. *Angew. Chem. Int. Ed.* **2021,** *60* (28), 15291-15295.
43. Zhang, Q.; Zhang, Y.-E.; Tong, S.; Wang, M.-X., Hydrocarbon Belts with Truncated Cone Structures. *J. Am. Chem. Soc.* **2020,** *142* (3), 1196-1199.

44. Smith, J. N.; Lucas, N. T., Rigid tetraarylene-bridged cavitands from reduced-symmetry resorcin[4]arene derivatives. *Chem. Commun.* **2018,** *54* (37), 4716-4719.

45. André, E.; Boutonnet, B.; Charles, P.; Martini, C.; Aguiar-Hualde, J.-M.; Latil, S.; Guérineau, V.; Hammad, K.; Ray, P.; Guillot, R.; Huc, V., A New, Simple and Versatile Strategy for the Synthesis of Short Segments of Zigzag-Type Carbon Nanotubes. *Chem. Eur. J.* **2016,** *22* (9), 3105-3114.

46. Mirzaei, S.; Castro, E.; Hernández Sánchez, R., Tubularenes. *Chem. Sci.* **2020,** *11* (31), 8089-8094.

47. Castro, E.; Mirzaei, S.; Hernández Sánchez, R., Radially Oriented [n]Cyclo-meta-phenylenes. *Org. Lett.* **2021,** *23* (1), 87-92.

48. Fan, G.; Zhang, Z.; Wang, G.; Shao, L.; Hua, B.; Huang, F., Construction of hydrocarbon belts based on macrocyclic arenes. *Chem. Sci.* **2024,** *15* (28), 10713-10723.

49. Tunstad, L. M.; Tucker, J. A.; Dalcanale, E.; Weiser, J.; Bryant, J. A.; Sherman, J. C.; Helgeson, R. C.; Knobler, C. B.; Cram, D. J., Host-guest complexation. 48. Octol building blocks for cavitands and carcerands. *J. Org. Chem.* **1989,** *54* (6), 1305-1312.

50. Merget, S.; Catti, L.; Piccini, G.; Tiefenbacher, K., Requirements for Terpene Cyclizations inside the Supramolecular Resorcinarene Capsule: Bound Water and Its Protonation Determine the Catalytic Activity. *J. Am. Chem. Soc.* **2020,** *142* (9), 4400-4410.

51. Hillyer, M. B.; Gibb, C. L. D.; Sokkalingam, P.; Jordan, J. H.; Ioup, S. E.; Gibb, B. C., Synthesis of Water-Soluble Deep-Cavity Cavitands. *Org. Lett.* **2016,** *18* (16), 4048-4051.

52. Srinivasan, K.; Gibb, B. C., Electrophilic Substitution of Deep Cavity Cavitands: Selective Exo Functionalization of Molecular Concavity. *Org. Lett.* **2007,** *9* (5), 745-748.

53. Becke, A. D., Density-functional thermochemistry. III. The role of exact exchange. *J. Chem. Phys.* **1993,** *98* (7), 5648-5652.

54. Phelan, N. F.; Orchin, M., Cross conjugation. *J. Chem. Educ.* **1968,** *45* (10), 633.

55. Limacher, P. A.; Lüthi, H. P., Cross-conjugation. *WIREs Comput. Mol. Sci.* **2011,** *1* (4), 477-486.

56. Valkenier, H.; Guédon, C. M.; Markussen, T.; Thygesen, K. S.; van der Molen, S. J.; Hummelen, J. C., Cross-conjugation and quantum interference: a general correlation? *Phys. Chem. Chem. Phys.* **2014,** *16* (2), 653-662.

57. Nishihara, T.; Segawa, Y.; Itami, K.; Kanemitsu, Y., Excited States in Cycloparaphenylenes: Dependence of Optical Properties on Ring Length. *J. Phys. Chem. Lett.* **2012,** *3* (21), 3125-3128.

58. Fujitsuka, M.; Cho, D. W.; Iwamoto, T.; Yamago, S.; Majima, T., Size-dependent fluorescence properties of [*n*]cycloparaphenylenes (*n* = 8–13), hoop-shaped π-conjugated molecules. *Phys. Chem. Chem. Phys.* **2012,** *14* (42), 14585-14588.

59. Segawa, Y.; Fukazawa, A.; Matsuura, S.; Omachi, H.; Yamaguchi, S.; Irle, S.; Itami, K., Combined experimental and theoretical studies on the photophysical properties of cycloparaphenylenes. *Org. Biomol. Chem.* **2012,** *10* (30), 5979-5984.

60. Talipov, M. R.; Jasti, R.; Rathore, R., A Circle Has No End: Role of Cyclic Topology and Accompanying Structural Reorganization on the Hole Distribution in Cyclic and Linear Poly-p-phenylene Molecular Wires. *J. Am. Chem. Soc.* **2015,** *137* (47), 14999-15006.

61. Kroto, H. W.; Heath, J. R.; O'Brien, S. C.; Curl, R. F.; Smalley, R. E., $C_{60}$: Buckminsterfullerene. *Nature* **1985,** *318* (6042), 162-163.

62. Sygula, A.; Fronczek, F. R.; Sygula, R.; Rabideau, P. W.; Olmstead, M. M., A Double Concave Hydrocarbon Buckycatcher. *J. Am. Chem. Soc.* **2007,** *129* (13), 3842-3843.

63. Pérez, E. M.; Martín, N., Molecular tweezers for fullerenes. *Pure Appl. Chem.* **2010,** *82* (3), 523-533.

64. Takeda, M.; Hiroto, S.; Yokoi, H.; Lee, S.; Kim, D.; Shinokubo, H., Azabuckybowl-Based Molecular Tweezers as $C_{60}$ and $C_{70}$ Receptors. *J. Am. Chem. Soc.* **2018,** *140* (20), 6336-6342.

65. Yang, Y.; Juríček, M., Fullerene Wires Assembled Inside Carbon Nanohoops. *ChemPlusChem* **2022,** *87* (1), e202100468.

66. Sun, Z.; Ikemoto, K.; Fukunaga Toshiya, M.; Koretsune, T.; Arita, R.; Sato, S.; Isobe, H., Finite phenine nanotubes with periodic vacancy defects. *Science* **2019,** *363* (6423), 151-155.

67. García-Simón, C.; Costas, M.; Ribas, X., Metallosupramolecular receptors for fullerene binding and release. *Chem. Soc. Rev.* **2016,** *45* (1), 40-62.

68. Brenner, W.; Ronson, T. K.; Nitschke, J. R., Separation and Selective Formation of Fullerene Adducts within an $M^{II}_8L_6$ Cage. *J. Am. Chem. Soc.* **2017,** *139* (1), 75-78.

69. Evans, D. R.; Fackler, N. L. P.; Xie, Z.; Rickard, C. E. F.; Boyd, P. D. W.; Reed, C. A., π-Arene/Cation Structure and Bonding. Solvation versus Ligand Binding in Iron(III) Tetraphenylporphyrin Complexes of Benzene, Toluene, p-Xylene, and [60]Fullerene. *J. Am. Chem. Soc.* **1999,** *121* (37), 8466-8474.

70. Boyd, P. D. W.; Hodgson, M. C.; Rickard, C. E. F.; Oliver, A. G.; Chaker, L.; Brothers, P. J.; Bolskar, R. D.; Tham, F. S.; Reed, C. A., Selective Supramolecular Porphyrin/Fullerene Interactions1. *J. Am. Chem. Soc.* **1999,** *121* (45), 10487-10495.

71. Olmstead, M. M.; Costa, D. A.; Maitra, K.; Noll, B. C.; Phillips, S. L.; Van Calcar, P. M.; Balch, A. L., Interaction of Curved and Flat Molecular Surfaces. The Structures of Crystalline Compounds Composed of Fullerene ($C_{60}$, $C_{60}O$, $C_{70}$, and $C_{120}O$) and Metal Octaethylporphyrin Units. *J. Am. Chem. Soc.* **1999,** *121* (30), 7090-7097.

72. Sun, D.; Tham, F. S.; Reed, C. A.; Chaker, L.; Burgess, M.; Boyd, P. D. W., Porphyrin−Fullerene Host−Guest Chemistry. *J. Am. Chem. Soc.* **2000,** *122* (43), 10704-10705.

73. Ishii, T.; Aizawa, N.; Kanehama, R.; Yamashita, M.; Sugiura, K.-i.; Miyasaka, H., Cocrystallites consisting of metal macrocycles with fullerenes. *Coordin. Chem. Rev.* **2002,** *226* (1), 113-124.

74. Zhang, C.; Wang, Q.; Long, H.; Zhang, W., A Highly $C_{70}$ Selective Shape-Persistent Rectangular Prism Constructed through One-Step Alkyne Metathesis. *J. Am. Chem. Soc.* **2011,** *133* (51), 20995-21001.

75. Leonhardt, V.; Fimmel, S.; Krause, A.-M.; Beuerle, F., A covalent organic cage compound acting as a supramolecular shadow mask for the regioselective functionalization of $C_{60}$. *Chem. Sci.* **2020,** *11* (32), 8409-8415.

76. Ni, Y.; Gordillo-Gámez, F.; Peña Alvarez, M.; Nan, Z.; Li, Z.; Wu, S.; Han, Y.; Casado, J.; Wu, J., A Chichibabin's Hydrocarbon-Based Molecular Cage: The Impact of Structural Rigidity on Dynamics, Stability, and Electronic Properties. *J. Am. Chem. Soc.* **2020,** *142* (29), 12730-12742.

77. Xu, Y.-Y.; Tian, H.-R.; Li, S.-H.; Chen, Z.-C.; Yao, Y.-R.; Wang, S.-S.; Zhang, X.; Zhu, Z.-Z.; Deng, S.-L.; Zhang, Q.; Yang, S.; Xie, S.-Y.; Huang, R.-B.; Zheng, L.-S., Flexible decapyrrylcorannulene hosts. *Nat. Commun.* **2019,** *10* (1), 485.

78. Wang, J.; Ju, Y.-Y.; Low, K.-H.; Tan, Y.-Z.; Liu, J., A Molecular Transformer: A π-Conjugated Macrocycle as an Adaptable Host. *Angew. Chem. Int. Ed.* **2021,** *60* (21), 11814-11818.

79. González-Delgado, A. M.; Giner-Casares, J. J.; Brezesinski, G.; Regnouf-de-Vains, J.-B.; Camacho, L., Langmuir Monolayers of an Inclusion Complex Formed by a New Calixarene Derivative and Fullerene. *Langmuir* **2012,** *28* (33), 12114-12121.

80. Zhang, F.; Du, X.-S.; Song, K.-Z.; Han, Y.; Lu, H.-Y.; Chen, C.-F., A calix[3]carbazole-based cavitand: synthesis, structure and its complexation with fullerenes. *Chem. Commun.* **2024,** *60* (37), 4962-4965.

81. Pfeuffer-Rooschüz, J.; Heim, S.; Prescimone, A.; Tiefenbacher, K., Megalo-Cavitands: Synthesis of Acridane[4]arenes and Formation of Large, Deep Cavitands for Selective $C_{70}$ Uptake. *Angew. Chem. Int. Ed.* **2022,** *61* (42), e202209885.

82. Chae, H. K.; Siberio-Pérez, D. Y.; Kim, J.; Go, Y.; Eddaoudi, M.; Matzger, A. J.; O'Keeffe, M.; Yaghi, O. M., A route to high surface area, porosity and inclusion of large molecules in crystals. *Nature* **2004,** *427* (6974), 523-527.

83. Goswami, S.; Ray, D.; Otake, K.-i.; Kung, C.-W.; Garibay, S. J.; Islamoglu, T.; Atilgan, A.; Cui, Y.; Cramer, C. J.; Farha, O. K.; Hupp, J. T., A porous, electrically conductive hexa-zirconium(iv) metal–organic framework. *Chem. Sci.* **2018,** *9* (19), 4477-4482.

84. Kawase, T.; Kurata, H., Ball-, Bowl-, and Belt-Shaped Conjugated Systems and Their Complexing Abilities: Exploration of the Concave−Convex π−π Interaction. *Chem. Rev.* **2006,** *106* (12), 5250-5273.

85. Matsuno, T.; Sato, S.; Isobe, H., 3.13 - Curved π-Receptors. In *Comprehensive Supramolecular Chemistry II*, Atwood, J. L., Ed. Elsevier: Oxford, 2017; pp 311-328.

86. Fuertes-Espinosa, C.; Pujals, M.; Ribas, X., Supramolecular Purification and Regioselective Functionalization of Fullerenes and Endohedral Metallofullerenes. *Chem.* **2020,** *6* (12), 3219-3262.

87. Steed, J. W.; Junk, P. C.; Atwood, J. L.; Barnes, M. J.; Raston, C. L.; Burkhalter, R. S., Ball and Socket Nanostructures: New Supramolecular Chemistry Based on Cyclotriveratrylene. *J. Am. Chem. Soc.* **1994,** *116* (22), 10346-10347.

88. Hardie, M. J.; Godfrey, P. D.; Raston, C. L., Self-Assembly of Grid and Helical Hydrogen-Bonded Arrays Incorporating Bowl-Shaped Receptor Sites That Bind Globular Molecules. *Chem. Eur. J.* **1999,** *5* (6), 1828-1833.

89. Suzuki, T.; Nakashima, K.; Shinkai, S., Very Convenient and Efficient Purification Method for Fullerene ($C_{60}$) with 5,11,17,23,29,35,41,47-Octa-*tert*-butylcalix[8]arene-49,50,51,52,53,54,55,56-octol. *Chem. Lett.* **1994,** *23* (4), 699-702.

90. S. Isaacs, N.; J. Nichols, P.; L. Raston, C.; A. Sandova, C.; J. Young, D., Solution volume studies of a deep cavity inclusion complex of $C_{60}$: [p-benzylcalix[5]arene⊂$C_{60}$]. *Chem. Commun.* **1997,** (19), 1839-1840.

91. Ogoshi, T.; Ueshima, N.; Sakakibara, F.; Yamagishi, T.-a.; Haino, T., Conversion from Pillar[5]arene to Pillar[6–15]arenes by Ring Expansion and Encapsulation of $C_{60}$ by Pillar[n]arenes with Nanosize Cavities. *Org. Lett.* **2014,** *16* (11), 2896-2899.

92. Atwood, J. L.; Barbour, L. J.; Raston, C. L., Supramolecular Organization of $C_{60}$ into Linear Columns of Five-Fold, Z-Shaped Strands. *Cryst. Growth & Des.* **2002,** *2* (1), 3-6.

93. Makha, M.; Raston, C. L.; Sobolev, A. N.; Turner, P., Exclusive Endo-Cavity Interplay of t-Bu-calix[6]arene with $C_{70}$. *Cryst. Growth & Des.* **2006,** *6* (1), 224-228.

94. Bähring, S.; Larsen, K. R.; Supur, M.; Nielsen, K. A.; Poulsen, T.; Ohkubo, K.; Marlatt, C. W.; Miyazaki, E.; Takimiya, K.; Flood, A. H.; Fukuzumi, S.; Jeppesen, J. O., Ionic manipulation of charge-transfer and photodynamics of [60]fullerene confined in pyrrolo-tetrathiafulvalene cage. *Chem. Commun.* **2017,** *53* (71), 9898-9901.

95. Chen, B.; Holstein, J. J.; Horiuchi, S.; Hiller, W. G.; Clever, G. H., Pd(II) Coordination Sphere Engineering: Pyridine Cages, Quinoline Bowls, and Heteroleptic Pills Binding One or Two Fullerenes. *J. Am. Chem. Soc.* **2019,** *141* (22), 8907-8913.

96. Ruoff, R. S.; Tse, D. S.; Malhotra, R.; Lorents, D. C., Solubility of fullerene ($C_{60}$) in a variety of solvents. *J. Phys. Chem.* **1993,** *97*, 3379–3383.

97. Thordarson, P., Determining association constants from titration experiments in supramolecular chemistry. *Chem. Soc. Rev.* **2011,** *40* (3), 1305-1323.

98. Lee, S.; Chen, C.-H.; Flood, A. H., A pentagonal cyanostar macrocycle with cyanostilbene CH donors binds anions and forms dialkylphosphate [3]rotaxanes. *Nat. Chem.* **2013,** *5* (8), 704-710.

99. Li, Y.; Pink, M.; Karty, J. A.; Flood, A. H., Dipole-Promoted and Size-Dependent Cooperativity between Pyridyl-Containing Triazolophanes and Halides Leads to Persistent Sandwich Complexes with Iodide. *J. Am. Chem. Soc.* **2008,** *130* (51), 17293-17295.

100. Kleinpeter, E.; Klod, S.; Koch, A., Endohedral and External Through-Space Shieldings of the Fullerenes C50, C60, C60-6, C70, and C70-6Visualization of (Anti)Aromaticity and Their Effects on the Chemical Shifts of Encapsulated Nuclei. *J. Org. Chem.* **2008,** *73* (4), 1498-1507.

101. Yamamoto, Y.; Tsurumaki, E.; Wakamatsu, K.; Toyota, S., Nano-Saturn: Experimental Evidence of Complex Formation of an Anthracene Cyclic Ring with C60. *Angew. Chem. Int. Ed.* **2018,** *57* (27), 8199-8202.

102. http://supramolecular.org/

103. Tashiro, K.; Aida, T., Metalloporphyrin hosts for supramolecular chemistry of fullerenes. *Chem. Soc. Rev.* **2007,** *36* (2), 189-197.

104. Pérez, E. M.; Martín, N., Curves ahead: molecular receptors for fullerenes based on concave–convex complementarity. *Chem. Soc. Rev.* **2008,** *37* (8), 1512-1519.

105. Chang, X.; Xu, Y.; Delius, M. v., Recent advances in supramolecular fullerene chemistry. *Chem. Soc. Rev.* **2024,** *53*, 47-83.

106. Nishio, M., CH/π hydrogen bonds in crystals. *CrystEngComm* **2004,** *6* (27), 130-158.

107. Janiak, C., A critical account on π–π stacking in metal complexes with aromatic nitrogen-containing ligands. *J. Chem. Soc. Dalton* **2000,** (21), 3885-3896.

108. Lu, T.; Chen, Q., Independent gradient model based on Hirshfeld partition: A new method for visual study of interactions in chemical systems. *J. Comput. Chem.* **2022,** *43* (8), 539-555.

109. H. Williams, D.; S. Westwell, M., Aspects of weak interactions. *Chem. Soc. Rev.* **1998,** *27* (1), 57-64.

110. Houk, K. N.; Leach, A. G.; Kim, S. P.; Zhang, X., Binding Affinities of Host–Guest, Protein–Ligand, and Protein–Transition-State Complexes. *Angew. Chem. Int. Ed.* **2003,** *42* (40), 4872-4897.

111. Yi, H.; Zeng, G.; Lai, C.; Huang, D.; Tang, L.; Gong, J.; Chen, M.; Xu, P.; Wang, H.; Cheng, M.; Zhang, C.; Xiong, W., Environment-friendly fullerene separation methods. *Chem. Eng. J.* **2017,** *330*, 134-145.

112. Morris, K. F.; Johnson, C. S., Jr., Diffusion-ordered two-dimensional nuclear magnetic resonance spectroscopy. *J. Am. Chem. Soc.* **1992,** *114* (8), 3139-3141.

113. Bezmel'nitsyn, V. N.; Eletskii, A. V.; Okun, M. V., Fullerenes in solutions. *Phys. Usp.* **1998,** *41* (11), 1091-1114.

114. Iloukhani, H.; Samiey, B., Studies of Viscosities and Excess Molar Volumes of the Binary Mixtures of 1-Heptanol + 1,2-Dichloroethane, + 1,1,1-Trichloroethane, + 1,1,2,2-Tetrachloroethane, + Trichloroethylene and Tetrachloroethylene at (293.15, 298.15, and 303.15) K for the Liquid Region and at Ambient Pressure. *J. Chem. Eng. Data* **2005,** *50* (6), 1911-1916.

115. Cameron, K. S.; Fielding, L., NMR diffusion coefficient study of steroid–cyclodextrin inclusion complexes. *Magn. Reson. Chem.* **2002,** *40* (13), S106-S109.

116. Oliva, A. I.; Gómez, K.; González, G.; Ballester, P., Diffusion-ordered spectroscopy (1H-DOSY) of Zn-porphyrin assemblies induced by coordination with DABCO. *New J. Chem.* **2008,** *32* (12), 2159-2163.

117. Ruzicka, E.; Pellechia, P.; Benicewicz, B. C., Polymer Molecular Weights via DOSY NMR. *Analytical Chemistry* **2023,** *95* (20), 7849-7854.

118. Carboni, A.; Emke, E.; Parsons, J. R.; Kalbitz, K.; de Voogt, P., An analytical method for determination of fullerenes and functionalized fullerenes in soils with high performance liquid chromatography and UV detection. *Anal. Chim. Acta* **2014,** *807*, 159-165.

119. Data obtained from Sigma-Aldrich Product Specification sheet: https://www.sigmaaldrich.com/specification-sheets/297/045/572497-BULK_____ALDRICH__.pdf Data accessed Sep 16, 2024.

120. Yamada, M.; Akasaka, T.; Nagase, S., Salvaging Reactive Fullerenes from Soot by Exohedral Derivatization. *Angew. Chem. Int. Ed.* **2018,** *57* (41), 13394-13405.

121. Wang, C.-R.; Shi, Z.-Q.; Wan, L.-J.; Lu, X.; Dunsch, L.; Shu, C.-Y.; Tang, Y.-L.; Shinohara, H., $C_{64}H_4$: Production, Isolation, and Structural Characterizations of a Stable Unconventional Fulleride. *J. Am. Chem. Soc.* **2006,** *128* (20), 6605-6610.

122. Han, X.; Zhou, S.-J.; Tan, Y.-Z.; Wu, X.; Gao, F.; Liao, Z.-J.; Huang, R.-B.; Feng, Y.-Q.; Lu, X.; Xie, S.-Y.; Zheng, L.-S., Crystal Structures of Saturn-Like $C_{50}Cl_{10}$ and Pineapple-Shaped $C_{64}Cl_4$: Geometric Implications of Double- and Triple-Pentagon-Fused Chlorofullerenes. *Angew. Chem. Int. Ed.* **2008,** *47* (29), 5340-5343.

123. Shan, G.-J.; Tan, Y.-Z.; Zhou, T.; Zou, X.-M.; Li, B.-W.; Xue, C.; Chu, C.-X.; Xie, S.-Y.; Huang, R.-B.; Zhen, L.-S., $C_{64}Cl_8$: A Strain-Relief Pattern to Stabilize Fullerenes Containing Triple Directly Fused Pentagons. *Chem. Asian J.* **2012,** *7* (9), 2036-2039.

124. Tian, H.-R.; Chen, M.-M.; Wang, K.; Chen, Z.-C.; Fu, C.-Y.; Zhang, Q.; Li, S.-H.; Deng, S.-L.; Yao, Y.-R.; Xie, S.-Y.; Huang, R.-B.; Zheng, L.-S., An Unconventional Hydrofullerene $C_{66}H_4$ with Symmetric Heptagons Retrieved in Low-Pressure Combustion. *J. Am. Chem. Soc.* **2019,** *141* (16), 6651-6657.

125. Gao, C.-l.; Abella, L.; Tan, Y.-Z.; Wu, X.-Z.; Rodríguez-Fortea, A.; Poblet, J. M.; Xie, S.-Y.; Huang, R.-B.; Zheng, L.-S., Capturing the Fused-Pentagon $C_{74}$ by Stepwise Chlorination. *Inorg. Chem.* **2016,** *55* (14), 6861-6865.

126. Simeonov, K. S.; Amsharov, K. Y.; Jansen, M., Connectivity of the Chiral $D_2$-Symmetric Isomer of $C_{76}$ through a Crystal-Structure Determination of $C_{76}Cl_{18}{\cdot}TiCl_4$. *Angew. Chem. Int. Ed.* **2007,** *46* (44), 8419-8421.

127. Ioffe, I. N.; Goryunkov, A. A.; Tamm, N. B.; Sidorov, L. N.; Kemnitz, E.; Troyanov, S. I., Fusing Pentagons in a Fullerene Cage by Chlorination: IPR $D_2$-$C_{76}$ Rearranges into non-IPR $C_{76}Cl_{24}$. *Angew. Chem. Int. Ed.* **2009,** *48* (32), 5904-5907.

128. Simeonov, K. S.; Amsharov, K. Y.; Krokos, E.; Jansen, M., An Epilogue on the $C_{78}$-Fullerene Family: The Discovery and Characterization of an Elusive Isomer. *Angew. Chem. Int. Ed.* **2008,** *47* (33), 6283-6285.

129. Wang, C.-R.; Sugai, T.; Kai, T.; Tomiyama, T.; Shinohara, H., Production and isolation of an ellipsoidal $C_{80}$ fullerene. *Chem. Commun.* **2000,** (7), 557-558.

130. Miyake, Y.; Minami, T.; Kikuchi, K.; Kainosho, M.; Achiba, Y., Trends in Structure and Growth of Higher Fullerenes Isomer Structure of C86 and C88. *Molecular Crystals and Liquid Crystals Science and Technology. Section A. Molecular Crystals and Liquid Crystals* **2000,** *340* (1), 553-558.

131. Wang, Z.; Yang, H.; Jiang, A.; Liu, Z.; Olmstead, M. M.; Balch, A. L., Structural similarities in Cs(16)-C86 and C2(17)-C86. *Chem. Commun.* **2010,** *46* (29), 5262-5264.

132. Khamatgalimov, A. R.; Kovalenko, V. I., Electronic structure and stability of C86 fullerene Isolated-Pentagon-Rule isomers. *International Journal of Quantum Chemistry* **2011,** *111* (12), 2966-2971.

133. Yang, H.; Beavers, C. M.; Wang, Z.; Jiang, A.; Liu, Z.; Jin, H.; Mercado, B. Q.; Olmstead, M. M.; Balch, A. L., Isolation of a Small Carbon Nanotube: The Surprising Appearance of $D_{5h}(1)$-$C_{90}$. *Angew. Chem. Int. Ed.* **2010,** *49* (5), 886-890.

134. Koenig, R. M.; Tian, H.-R.; Seeler, T. L.; Tepper, K. R.; Franklin, H. M.; Chen, Z.-C.; Xie, S.-Y.; Stevenson, S., Fullertubes: Cylindrical Carbon with Half-Fullerene End-Caps and Tubular Graphene Belts, Their Chemical Enrichment, Crystallography of Pristine $C_{90}$-$D_{5h}(1)$ and $C_{100}$-$D_{5d}(1)$ Fullertubes, and Isolation of $C_{108}$, $C_{120}$, $C_{132}$, and $C_{156}$ Cages of Unknown Structures. *J. Am. Chem. Soc.* **2020,** *142* (36), 15614-15623.

135. Liu, X.; Bourret, E.; Noble, C. A.; Cover, K.; Koenig, R. M.; Huang, R.; Franklin, H. M.; Feng, X.; Bodnar, R. J.; Zhang, F.; Tao, C.; Sublett, D. M., Jr.; Dorn, H. C.; Stevenson, S., Gigantic $C_{120}$ Fullertubes: Prediction and Experimental Evidence for Isomerically Purified Metallic [5,5] $C_{120}$-$D_{5d}(1)$ and Nonmetallic [10,0] $C_{120}$-$D_{5h}(10766)$. *J. Am. Chem. Soc.* **2022,** *144* (36), 16287-16291.

136. Yang, H.; Jin, H.; Che, Y.; Hong, B.; Liu, Z.; Gharamaleki, J. A.; Olmstead, M. M.; Balch, A. L., Isolation of Four Isomers of $C_{96}$ and Crystallographic Characterization of Nanotubular $D_{3d}(3)$-$C_{96}$ and the Somewhat Flat-Sided Sphere $C_2(181)$-$C_{96}$. *Chem. Eur. J.* **2012,** *18* (10), 2792-2796.

SYNOPSIS TOC